



Cite this: *J. Mater. Chem. B*, 2015, **3**, 5352

Fabrication of conductive polyaniline hydrogel using porogen leaching and projection microstereolithography†

Yibo Wu, Yong X. Chen, Jiahan Yan, Shihao Yang, Ping Dong and Pranav Soman*

Conducting hydrogels represent a new generation of “smart” biomaterials which combine the favorable biocompatibility properties of hydrogels and electrical properties of organic conductors, and would potentially lead to the development of new biointerfaces with controllable properties. Currently, conductive hydrogels are synthesized by either adding conducting particles to, or polymerizing conducting polymer monomers within, hydrogel matrix, however challenges in processing limit their applications in functional devices. In this work, a poly(ethylene glycol) diacrylate–polyaniline (PEGda–PANI) conductive hydrogel is developed using interfacial polymerization process. In this process, aniline monomers polymerize at the organic/water interface between hexane media and hydrophilic PEGda hydrogel networks. PANI chains become hydrophilic with acid doping and migrate into aqueous phase confined within PEGda networks. The synthesized PEGda–PANI hydrogel has acceptable mechanical, electrical and biocompatible properties. Traditional fabrication methods including process-driven salt-leaching and design-driven projection stereolithography were used to develop 3D scaffolds using PEGda–PANI hydrogels. This methodology can be potentially extended to a wide variety of fabrication techniques to develop hydrogels with complex geometries and next-generation functional biointerfaces.

Received 6th April 2015,
Accepted 2nd June 2015

DOI: 10.1039/c5tb00629e

www.rsc.org/MaterialsB

1. Introduction

Electric fields play a crucial role not only in the function of excitable tissues (nerves and muscles) but also in modulating cellular function such as proliferation, morphology, gene expression, migration and differentiation in a variety of cell types.^{1–5} As a result, researchers have sought to develop new biocompatible yet conductive materials to create a bioelectrical interface, which would promote transfer of electric signal in sensitive tissues and cells and in regenerative medicine, bio-robotics, and biosensing.⁶ Hydrogels which form 3D cross-linked fibers, have emerged as the ideal matrix for cell-culture and developing tissue scaffolds because of their hydrated nature, their permeability to oxygen, nutrient growth factor, metabolic waste, as well the flexibility of incorporating mechanical and biochemical cues.^{7–9} However, hydrogel are typically mechanically weak and electrically non-conductive, limiting their applications. Recently, conductive hydrogels have been developed by incorporating conducting elements such as graphite,¹⁰ metallic

particles,^{11,12} or carbon nanotubes^{11,13–15} within its matrix. However, in this approach, as conductive elements are typically randomly distributed within hydrogel matrix, a relatively large amount of conductive element are needed to form a continuous electrically-conductive network based on the percolation limit. Moreover, natural swelling response of hydrogel often can severely suppresses the conductivity of the system. Another approach of developing conductive hydrogel is to integrate inherently conductive polymers within the hydrogel matrix.

Conductive polymers such as poly(pyrrole) (PPy), poly(3,4-ethylenedioxythiophene) (PEDOT) and polyaniline (PANI), with their ability to conduct electricity due to the presence of conjugated double bonds or aromatic rings,¹⁶ have been used in a range of biomedical applications such as neural interfaces,^{6,17} electrochemical and bio-sensors,¹⁸ actuators, drug release,¹⁹ electrode coating and tissue scaffolds for regenerative medicine.^{20,21} PANI finds wide applications in biomedical engineering because of its unique combination of environmental stability and ease of synthesis.^{20,22} However its poor solubility in common organic solvent and limited fusability due to rigid macromolecular chains results in significant processing challenges to develop thin films as well as 3D structures, thereby severely limiting its use in developing functional bio-electric interfaces.²³ Integration of PANI within hydrogel matrix allows favorable characteristics of hydrogels such as soft elastic

Department of Biomedical and Chemical Engineering, Syracuse University,
900 S Crouse Ave, Syracuse, NY 13210, USA. E-mail: psoman@syr.edu;
Tel: +1 315-443-9322

† Electronic supplementary information (ESI) available. See DOI: 10.1039/c5tb00629e

material properties and high swelling ratio, to minimize mismatch at the interface with biological cells and tissues, and facilitate transport of nutrients, drugs and metabolites. However as PANI insolubility in common solvents along with brittle nature due to rigid π -conjugated bonds seriously hinders its use with standard fabrication techniques to develop functional devices.²³

Typically, thin PANI films developed using variety of methods, including electrochemical deposition, spin-casting,²⁴ self-assembly,²⁵ electrospinning,²⁶ and Langmuir–Blodgett methods,²⁷ and inkjet printing.^{28,29} However, for tissue engineering application, we need to go beyond thin films to develop 3D hydrogel scaffolds. In this work, we focus on developing bulk conductive hydrogel by combining interfacial polymerization of aniline monomers with a process-driven and a design-driven fabrication approach. We combine interfacial polymerization with (a) a process-driven porogen (salt)-leaching approach, and (b) a design-driven projection stereolithography, to fabricate conductive PEGda–PANI structures. This methodology with commonly used manufacturing approach has the advantage of design and fabrication flexibility, low cost, high-speed and user-defined patterning. This approach has the potential to be extended to a wide variety of synthetic and naturally-derived hydrogels.

2. Results and discussion

Crosslinked hydrogels are mesh-like hydrophilic structures with high water content and space in which another polymer can readily crosslink. We use poly(ethylene glycol) diacrylate hydrogel (PEGda) and subsequently use interfacial polymerization to crosslink polyaniline structure within its network. In this work, we follow a three step process. Step 1 utilizes UV photocrosslinking to develop a PEGda hydrogel (Fig. 1A). Liquid PEGda monomer solution mixed with photoinitiator is filled in a Teflon mold to form a disc shaped crosslinked PEGda hydrogel sample. In step 2, the PEGda sample is immersed in a solution of ammonium persulphate (APS-oxidant) dissolved in 1 M hydrochloric acid (HCL) (Fig. 1B). In step 3, the PEGda sample is immersed in a solution of aniline monomer dissolved in an organic solvent (hexane). Polymerization occurs at the hydrophilic PEGda/organic-solvent interface, as the aniline monomers transfer into the aqueous phase and self-assemble within the hydrogel network. The PANI chains located along the PEGda chains are simultaneously doped by HCL during the interfacial polymerization process. As polyaniline is hydrophilic in its doped state, it spontaneously migrates into the aqueous phase and is confined within the PEGda hydrogel matrix. Selective polymerization of aniline around PEGda backbone (a) prevents leaching out of newly synthesized PANI into the solution, and (b) prevents blocking of surface of bulk hydrogel by constant diffusion of newly synthesized PANI and APS into and out of PEGda matrix respectively, thereby leading to formation of hybrid conductive-hydrogel.³⁰

Typically, hydrogel-conductive polymer composites reported in the literature result in a phase separated conductive elements

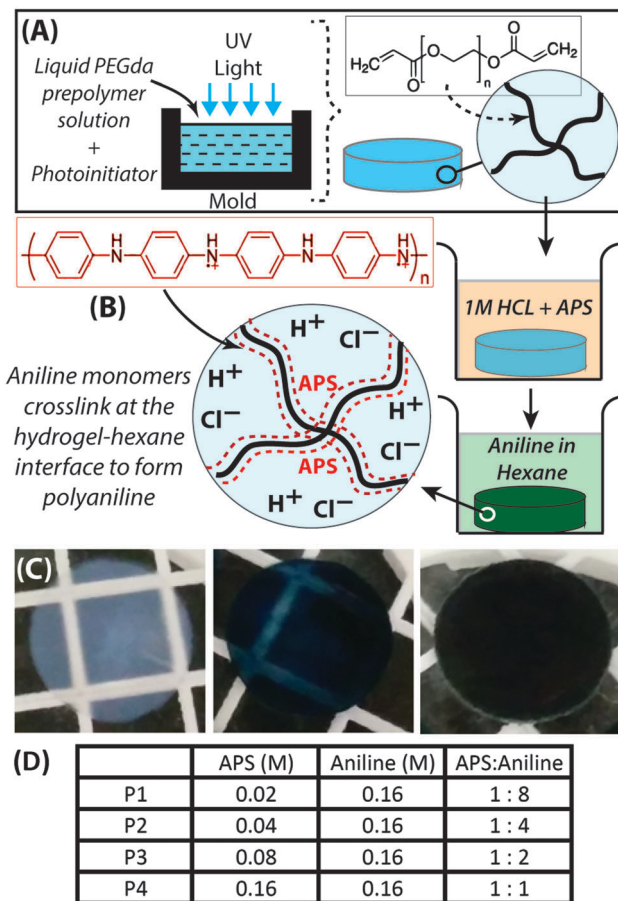


Fig. 1 Synthesis and formation of poly(ethylene glycol)-polyaniline (PEGda–PANI) conductive hydrogels using interfacial polymerization process. (A) PEGda monomers are crosslinking within a mold by UV crosslinking process. (B) PEGda samples are immersed in ammonium persulphate (APS-oxidant) in HCL solution, and subsequently transferred to a vial containing aniline in hexane (organic solvent). Aniline monomer polymerize to form polyaniline (PANI) at the water–hexane interface. Hydrophilic PANI spontaneously and exclusively assembles onto the hydrophilic PEGda matrix. (C) Transparent PEGda sample becomes opaque (dark-green color) with the formation of PANI within its matrix. The three picture show PEGda samples immersed in hexane + aniline solution for 0, 30 s and 3 minutes. Samples progressively get darker (dark-green) with formation of PANI within PEGda matrix. (D) Table lists various ratios of APS and aniline used in this work. Scale bar: 5 mm.

concentrated on the surface, and not integrated within the hydrogel structure.^{31–33} For example, conductive hydrogels developed on electrodes using electropolymerization, a commonly used technique, result in poor integration of the conductive element with the hydrogel structure. Another commonly used approach is to mix PANI with PEGda precursor solution, and crosslink the mixture using UV photopolymerization to create crosslinked hydrogel network.³⁴ This approach is particularly popular in biomedical applications because of its capability to encapsulate living cells, as well as flexibility of incorporating cell adhesion and proteolytic sites to induce specific cellular responses. However, this approach is highly dependent on the amount of nanoparticles, as even 3% NP (by weight) make the mixture opaque to UV light and decrease the crosslink density,

resulting in significant loss of PANI phases. In contrast, interfacial polymerization process,³⁰ used in this work, facilitates assembly of PANI exclusively within the crosslinking hydrogel network to facilitate obtain a PEGda–PANI composite.

The PEGda–PANI composite was thoroughly washed by DI water for 3 days and HCL for another 2 days, to allow any uncrosslinked PANI, residual APS to leach out. Transparent PEGda sample becomes opaque with the formation of the PANI (dark-green color) (Fig. 1C). In this work, we vary the ratio of aniline monomers and APS (Fig. 1D), and evaluate swelling ratios, compressive modulus and electrical properties. We choose to change the ratio of APS vs. aniline by increasing amounts of aniline. APS concentration never exceeded aniline concentration to prevent over-oxidation of PANI, as in case of PANI, only half-oxidized state (emeraldine salt) is conductive.

Characterization of PEGda–PANI

FTIR spectra of the PEGda and PEGda–PANI (P3) were recorded using Spectrum One FTIR Spectrometer from Perkin Elmer Instrument (Fig. 2A). We observe a small but distinct change in peaks occurring at 1141, and 1570 which represent the in-plane bending of C–H in aromatic moieties, and C=C stretching deformation of quinoid ring. The small changes in the peaks could be attributed to a relatively small amount of PANI within PEGda chains. As swelling ratio would influence the diffusion properties of media, we quantified mass swelling ratio of hydrogels for both PEGda (C1, C2) and PEGda–PANI (P1, P2, P3 and P4) samples, after incubating them in DI water for 3 days (Fig. 2B and ESI-1†). Swelling ratio of PEGda–PANI samples are similar to the C1 control (PEGda), however we observe a slight decrease in swelling ratio for P3 and P4 samples when compared to C2 (PEGda immersed into 1 M HCL solution). Minimal PEGda swelling observed in these samples also prevents leaching of PANI and thus minimize possible toxic effects and a drop in conductive properties as observed in studies with

high swelling ratios.³⁵ Moreover PANI does not neutralize due to disassociation of ionic interactions as the hydrogel matrix swells, a phenomenon often observed in ionically bound conductive hydrogels.³⁶

Since it is well accepted that stiffness significantly influences cell-materials interactions, we quantified the changes in compressive modulus of PEGda–PANI (P3) at various stages of the process using Dynamic Mechanical Analyzer (Q800, TA Instruments). 3D disc samples (16 mm in diameter and 1.62 mm in thickness) were used for this study. Samples loaded under compression clamp and the slope of stress–strain curve from 0–10% strain (Fig. 2C) was used to determine the modulus. PEGda control sample without any PANI was chosen as the control with stiffness value of 66.9 ± 5.1 kPa. As the sample goes through the various steps of the process, we observe a statically insignificant decrease in its modulus to a value of 54.4 ± 4 kPa (Fig. 2C and ESI-1†). From the results, we find no significant difference between the C1 PEGda samples and the PEGda–PANI (P3) samples, and conclude that the interfacial polymerization process does not significantly alter the compressive modulus. Similar to swelling ratio, modulus of P3 and P4 samples are significantly different than C2 control sample (PEGda immersed in HCL). PEGda–PANI samples even with high aniline concentration (mass fraction) still results in a small decrease in its compressive modulus (Fig. 2C). For example, P1 sample with the highest concentration of aniline has a modulus of 48 ± 1.9 kPa. This is in contrast to other methods of developing conductive hydrogels, such as doping hydrogels with nanowires and other conductive elements to make a conductive hydrogel, which typically results in an increase in the modulus within the physiological range of stiffness of various cell types (1 kPa to 100 kPa),³⁷ will be useful in developing effective bioelectronic interfaces that fully recapitulate the biomechanical responses of *in vivo* cells and tissues. Moreover, several methods

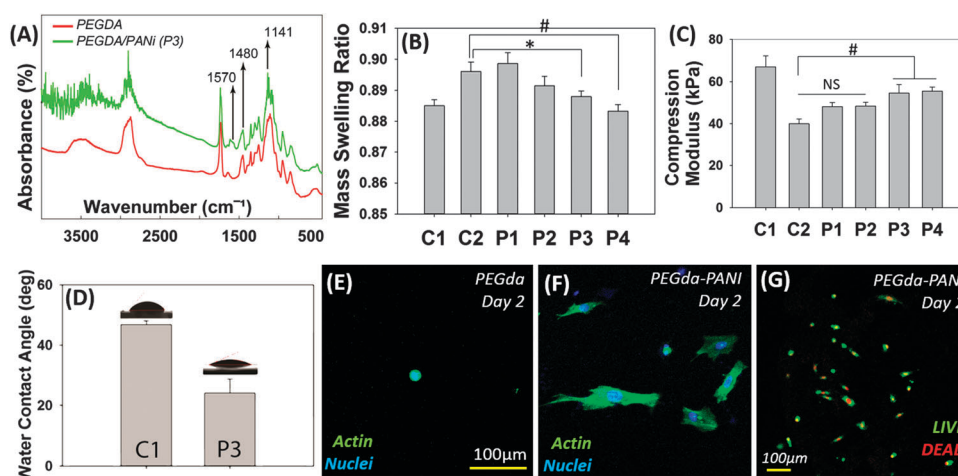


Fig. 2 Material characterization of PEGda and PEGda–PANI samples: (A) FTIR analysis showing peaks at 1141, 1480 and 1570 cm^{-1} , mass swelling ratio (B) and compressive modulus (C) for various samples. (D) Contact angle analysis. (E and F) Morphology of murine mesenchymal progenitor (10T1/2) cells as depicted by stained for F-actin (green) and nuclei (blue) 2 days post-seeding. (G) Representative image of viability of 10T1/2 cells seeded on PEGda–PANI samples as assessed *via* calcein-AM (green)/ethidium homodimer (red) assay 2 days post-seeding. (Control PEGda samples: C1 is PEGda without any further processing; C2 is PEGda sample immersed in HCL but not in aniline solution.)

to modulate the stiffness of hydrogels, including changing molecular weight or degree of crosslinking, can be used to develop PEGda-PANI with a wide range of stiffnesses.

Biocompatibility of PEGda-PANI

C3H/10T1/2 murine mesenchymal progenitor cells (10T1/2s) were seeded on both PEGda and PEGda-PANI (P3) samples with a final concentration of 1.22×10^5 cells per mL. At day 2 post-seeding, results demonstrate higher cell spreading and good cell viability on PEGda-PANI. The green fluorescent dye calcein indicated viable cells, and red nuclei showed damaged and dead cells with the membrane-dye Eth-D1. Contact angle of P3 was found to be lower (more hydrophilic) as compared to C1 PEGda control, which was expected as PANI doped by HCL acid becomes hydrophilic. The increased cell-spreading could be attributed to increased protein adsorption to the half-oxidized emeraldine salt state of PANI. Overnight incubation of samples also support physioadsorption of proteins resulting in cell spreading at day 2 (as well as day 7-not shown here) indicated by elongated morphology of cells labeled for F-actin and nucleus. These results were similar to several reports in the literature, which demonstrate proliferation and adhesion of neural cells^{38,39} and cytocompatibility with cardiac myoblasts without any inflammation in rodent models.⁴⁰

Electrical characterization of PEGda-PANI

Conventional 4-probe conductivity measurements did not lead to reproducible results because of the weak electrical contact on the soft samples. We used Electrochemical Impedance Spectroscopy (EIS) to characterize the electrical properties of PEGda-PANI samples by fitting the experimental data with a standard Randles cell (RC) equivalent circuit models, and derived

polarization resistance and capacitance values. EIS measures the electrochemical responses of samples to a small AC voltage around the open circuit potential (OCP) of the test-sample, applied over a range of frequencies between 0.02 Hz and 20 kHz and an amplitude of the applied voltage was 10 mV. The data were fitted to an equivalent circuit using instant fit function available in ZView software. EIS spectra is plotted as Nyquist diagram with imaginary part ($-Z''$) plotted against the real component (Z'), where time constants from the equivalent circuit appears as a semicircle (Fig. 3A). The equivalent circuit composed a capacitance element (CPE) which replaces the ideal double layer capacitance, R_s , the uncompensated solution resistance and R_p , polarization resistance (inset in Fig. 3B). CPE represents the reaction step when electrons/ions build up on a surface, while a resistor represents the transport of charge through materials or interfaces. Since the phase angle for PEGda-PANI samples is ~ 70 , the capacitor element is treated as a constant phase element (CPE), modeled as a capacitor with a distribution of relaxation times. (Ideal capacitor should have a phase angle of -90 .) Nyquist plots also suggested that the impedance was dominated by a constant phase element (CPE) that can be represented by $CPE = 1/[A(j\omega)R]$ where A and R are constants, related to the phase angle. The dispersion of the plots can be attributed to defects and pore sizes in the sample or the interface. As all samples have only one time constant (only one peak is observed in Fig. 3A), a single CPE element would suffice. The best fit parameters are shown in supplementary section, and the fit is displayed in Nyquist format in Fig. 3A. The non-linear capacitance exhibited by PEGda-PANI composites could be attributed to either non-uniform diffusion and/or defects in PANI polymerization around PEGda chains.

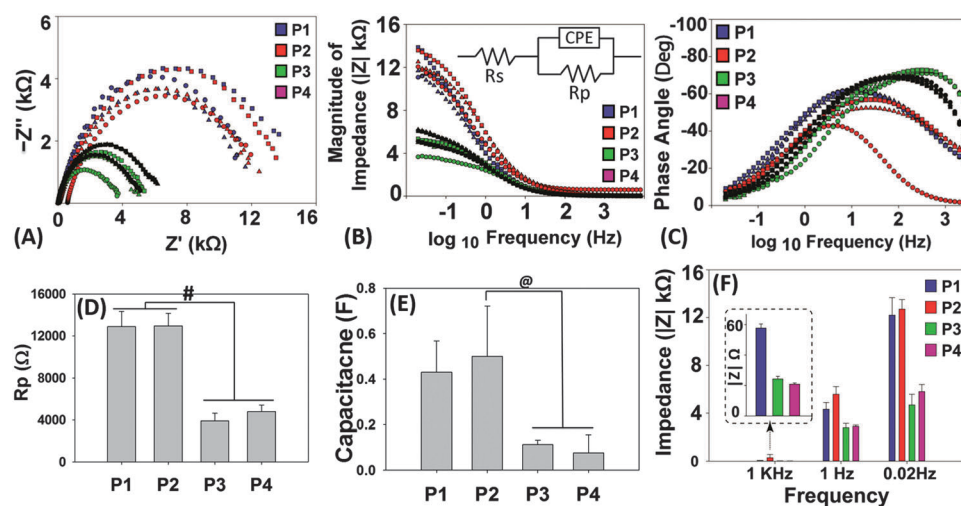


Fig. 3 Electrical characterization of PEGda-PANI hydrogels with varying ratio of aniline and APS using electrochemical impedance spectroscopy. (A) The full spectrum regime of Nyquist plots shown as a function of aniline : APS ratio. The data were fitted to an equivalent circuit composed a capacitance element (CPE), R_s , the uncompensated solution resistance and R_p , polarization resistance. With an increase in aniline (P4 to P1), the diameter of the semi-circle (time-constants) is observed to increase, indicating higher resistance to mass transfer. Bode plots showing the magnitude of impedance (B) and the phase angle (C) are plotted for frequencies f between 0.01 Hz and 10 kHz. Time constants from the equivalent circuit appears as a peak in the phase angle (C). (D–F) Values of polarization resistance, capacitance and impedance are plotted as a function of decreasing amount of aniline (P1 to P4). PEGda-PANI samples: P1 = blue; P2 = red; P3 = green and P4 = black. (#: $p < 0.001$; *: $p < 0.01$; @: $p < 0.05$; NS: no significant difference).

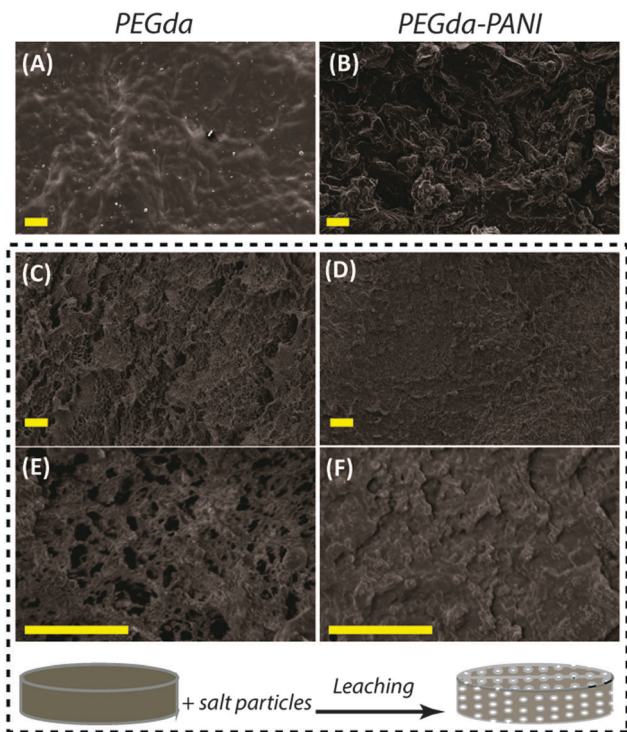


Fig. 4 Process-driven fabrication using salt-leaching approach was used. Scanning electron microscopy (Joel 5600, Japan) was used to image PEGda and PEGda-PANI samples. All samples were freeze-dried, sputter coated for 45 seconds, and mounted on an aluminum SEM stubs with double-sided carbon tape and imaged at 10 kV. (A) PEGda, (B) PEGda-PANI, (C, E) PEGda salt-leached, (D, F) PEGda-PANI salt leached. All scale bars are 100 μm .

EIS are also plotted as Bode diagrams, where the phase angle and modulus are plotted as functions of frequency, and

time constants from the equivalent circuit appears as a peak in the phase angle (Fig. 3B). Fig. 3B and C depicting the magnitude and the phase angle exhibit a well-defined time constant at lower frequencies, which can be seen by the peak in the phase angle plot. PEGda-PANI samples appears to have a single peak, which move toward high frequencies with decrease in aniline concentration (Fig. 3D-F). Electrical properties of PEGda-PANI samples were dependent on amount of aniline during *in situ* polymerization. P3 and P4 samples exhibited lower polarization resistance, capacitance and overall impedance as compared to P1 and P2 high-aniline concentration samples. Impedance also depends on the frequency (Fig. 3F), with an increase in impedance at lower frequencies: for example, P3 sample exhibited impedance of ~ 4 k Ω , 3 k Ω and 0.02 k Ω at 0.02, 1 and 1000 Hz. P3 sample has the optimal ratio of APS and aniline monomers, to achieve least impedance with minimal amount of oxidant (APS) which could result in over-oxidation of PANI. P3 sample was chosen to undergo a typical process-driven and design-driven fabrication methodology.

Process-driven approach: porogen leaching. We used a commonly used process-driven fabrication approach, salt-leaching technique to prepare PEGda-PANI porous hydrogels by leaching out sodium chloride crystals. Scanning electron microscopy (SEM) images (Fig. 4) taken from the cross-section of both PEGda and PEGda-PANI samples with and without the salt-leaching process demonstrate the presence of micropores, and the impregnation of polyaniline monomer within PEGda matrix. As salt dissolves and leaches out of the PEGda samples, micropores are created as demonstrated by Fig. 3C and E. After aniline polymerization within PEGda matrix, the micropores tend to get filled with PANI and influences the pore-morphology (Fig. 3D and F). This methodology can be extended to several

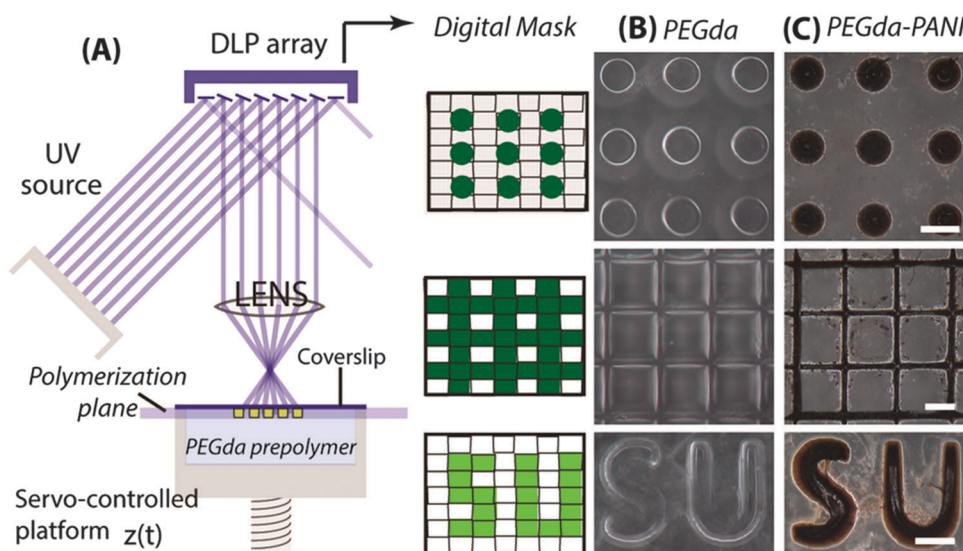


Fig. 5 Design-driven fabrication approach to develop PEGda-PANI samples: (A) schematic of projection stereolithography process. PEGda monomer solution is placed in a chamber covered by a methacrylated glass coverslip. Computer aided design (CAD) files with different digital masks were used to generate a series of virtual masks (dot, grid and letter patterns). Polymerization of the 3D scaffold begins at the coverslip surface, where UV light modulated by DLP array is focused. (B and C) Crosslinked PEGda and PEGda-PANI microstructures adhered to silanized glass coverslip are visualized using HIROX instrument. All scale bars are 200 μm .

established process-driven techniques including freeze-drying, particulate leaching, gas foaming and combinations to generate a wide range of conductive porous scaffolds.^{41–45} These approaches typically result in more or less random process-dependent porous structures, user-defined structures cannot be controlled. In the next section, we demonstrate that this methodology can be extended to design-driven techniques such as stereolithography.

Design-driven approach. Projection stereolithography (micro-stereolithography) systems has been used to fabricate microstructures using UV-sensitive resin mixed with typically non-biocompatible absorbers and quenchers.^{46–49} In this work, we used this system to develop conductive hydrogels in user-defined patterns. The main components of this system is a digital micro-mirror projection (DLP) array (Texas Instruments) which can be loaded with any user-defined bitmap files to make virtual digital masks, which selectively switch mirrors into either the ON state or the OFF state (Fig. 5A). The ON state reflects the UV light into the focusing lens, which projects the image into the liquid prepolymer solution, while the OFF state diverts the UV light away from the prepolymer solution. Using this approach, we develop three user-defined patterns in PEGda hydrogels, a dot pattern, an intersecting square grid, and a letter symbol SU representing Syracuse University (Fig. 5B). These samples underwent the interfacial polymerization process to impregnate the PEGda network with aniline monomers to form a hybrid conductive PEGda–PANI. We chose P3 as our ratio, indicated by dark-green (almost black) structures (Fig. 5C). This methodology can be extended to other design-driven approaches such as inkjet printing, fused deposition modeling and direct laser writing, to develop new conductive hydrogel scaffolds with specific 3D geometry.^{50–53}

3. Conclusions

In this work, we design and develop biocompatible PEGda–PANI scaffolds using interfacial polymerization. In this process, PANI formed at the water/organic-solvent interface (PEGda/hexane) migrates within PEGda matrix resulting in a homogenous network of conductive hydrogels. We also demonstrate that there is little change in the mass swelling and compressive modulus of PEGda–PANI samples as compared to PEGda control which is essential for developing new biomimetic electrical interfaces. In this work, we demonstrate how commonly used fabrication techniques can be utilized to develop conductive hydrogel with new complex geometries. First we choose a process-driven porogen-leaching method, to fabricate PEGda–PANI scaffolds with micropores. Second, we choose a design-driven projection stereolithography to print dot, grid and letter patterns in PEGda–PANI at micron resolutions. By combining already existing wide range of fabrication techniques with interfacial polymerization, new conductive hydrogels of synthetic/natural origin with complex geometries can be developed. This approach is broadly applicable for a variety of hydrogel systems, and can be potentially used to engineer new hybrid bioelectronics interface for several biomedical applications.

4. Experimental section

Preparation of conductive hydrogels

Poly(ethylene glycol) diacrylate (PEGda – 700 MW) prepolymer solution was prepared using 10% PEGda (v/v) and 0.25% Irgacure 2959 photoinitiator. A rectangular mold, using Teflon sheet clamped between two glass slides, was used to prepare hydrogel sheet (thickness 1.6 mm). UV light (Omniscure S2000, exposure time: 10 min) was used to crosslink PEGda prepolymer solution. A circular punch was used to make disc shaped PEGda samples (diameter = 16 mm). PEGda samples were stored in DI water for one day to remove impurities. PEGda samples were immersed in 0.02, 0.04, 0.08 and 0.16 M ammonium persulfate (APS) in 1 M HCL solution (refer to Fig. 1D) for 4 hours, and subsequently immersing the samples into aniline solution in hexane for 4 hours. Aniline monomers polymerize within the PEGda chains to form a PEGda–PANI hybrid samples. Samples were purified in large amount of DI water for 3 days and 1 M HCL for another 2 days, to ensure removal of residual aniline monomers and APS.

Electrochemical Impedance Spectroscopy (EIS)

The electrical conductivity of PEGda–PANI hydrogel samples were measured by EIS at frequencies from 0.02 Hz to 20 000 Hz and AC perturbation of 10 mV. Basically, a disk shaped PEGDA/PANI samples were placed in an electrode system between a Titanium electrode and a hole (diameter – 8 mm). Ag/AgCl and carbon electrodes were used as the reference and counter electrodes respectively, while 1 M H₂SO₄ solution was used as the electrolyte (ESI-2†). This three electrode cell was connected to a Solartron Analytical 1280Z working station to drive electrochemical impedance spectroscopy test. Data was collected and analyzed by Z plot and Z view software respectively.

Swelling ratio

PEGda–PANI hydrogel samples (diameter 16 mm, thickness 1.62 mm) with different ratios (Fig. 1D) were incubated in DI water for 3 days and dried overnight at room temperature. The swelling ratio was measured by comparing the swollen weight over the dried weight, as follows: swelling ratio (%) = $((W_w - W_i)/W_w) \times 100\%$ (W_w : wet weight of hydrogel; W_i : initial [dry] weight of hydrogel sample).

Compressive modulus

Compressive modulus was quantified using a Q800 Dynamic Mechanical Analysis (DMA) (TA Instruments, Inc.). Disc-shaped PEGda–PANI samples (diameter 16 mm, thickness 1.62 mm) of different ratios were incubated in phosphate buffer saline (PBS) at 37 °C for 48 hours. Samples were loaded under compression clamp and tested for controlled strain percentage (ramping from 0–40%) with preloaded force of 0.01 N and displacement of 10 μm. The slope of stress–strain curve from 0–10% strain was used to determine compressive modulus.

Cell culture and immunohistochemical staining

C3H/10T1/2 murine mesenchymal progenitor cells (10T1/2s), generously gifted by Dr Henderson, were cultured in BME supplemented with 10% fetal bovine serum, 1% Glutamax, 1% Penstrap, and were maintained in a 37 °C incubator with 5% CO₂. Cells were passaged using standard cell culture protocols using 0.25% trypsin–EDTA and were used within passage number 15. Cells were harvested, counted and seeded on PEGda or PEGda–PANI samples, media was changed 1 day after seeding and then refreshed every other day. Cells were fixed on day 2, post-seeding using 4% paraformaldehyde (Invitrogen, Carlsbad, CA) overnight at room temperature and permeabilized with 0.1% Triton X-100 (Sigma-Aldrich) in PBS with 1% bovine serum albumin (BSA, Hyclone) for 30 min. For F-actin and nuclei staining cells were labeling secondary antibodies (Alexa 488 or Alexa 647, Invitrogen, Carlsbad, CA) and Hoechst 33258 DNA dye (Invitrogen, Carlsbad, CA) for 30 minutes. Confocal fluorescence imaging was performed using Zeiss LSM 710, and image analysis was performed using ImageJ.

Contact angle

The water contact angle measurements of PEGDA–PANI and PAGDA were performed using VCA Optima (AST Products, Inc.). A drop of DI water (0.75 µl) was placed on the surface of the sample and images of the water menisci were recorded by a digital camera. For each type of sample, 8 independent samples were tested.

SEMs

PEGda and PEGda–PANI samples were imaged using Scanning Electron Microscopy (Joel 5600, Japan). Samples were cut in half, freeze-dried, sputter coated for 45 seconds, and mounted on an aluminum SEM stubs with double-sided carbon tape and imaged using 5 kV.

Porogen leaching

Sodium chloride crystals with 20% volume concentration were added to PEGda prepolymer solution, and exposed to UV light (EXFO Omnicure S2000, Quebec, QC, Canada) for 10 min to form disc-shaped PEGda + salt samples of standard size (diameter 16 mm, thickness 1.62 mm). Samples were incubated in DI water for 3 days to facilitate salt-leaching, following by interfacial polymerization of aniline monomers as described previously.

Methacrylation of glass coverslips

Round glass coverslips (12 mm Dia, Chemglass Life Sciences, Vineland, NJ) were agitated in Piranha solution (sulfuric acid and hydrogen peroxide at a 7:3 ratio) for 5 min, washed in DI water 3× (5 min each time), and washed in 100% ethanol (Fisher Scientific, Pittsburgh, PA) and dried with nitrogen. Dried glass coverslips were functionalized in a bath containing 85 mM 3-(trimethoxysilyl)propyl methacrylate (Fluka, St. Louis, MO) in ethanol with acetic acid (pH 4.5) with overnight rocking at room temperature. Modified coverslips were washed with

ethanol (5×, 5 min each wash cycle), dried with nitrogen, and baked in oven for 1 h.

Projection stereolithography

Three micron-scale user-defined patterns were fabricated using PEGda hydrogel using UV photolithography in a layer-by-layer fashion. The main components of the fabrication system are a UV light source (EXFO Omnicure S2000, wavelength range 320–500 nm, Quebec, QC, Canada), a digital light processing (DLP) chip (Discovery 4000, Texas Instrument, TX), and computer controlled stages (Newport 426/433 series). User-defined computer-aided-design (CAD) files of dot, grid and letter patterns were transferred to the DLP array chip to generate a series of virtual masks. DLP chip modulated images were projected onto a photocurable pre-polymer through an UV grade optical lens (Edmunds Optics, NJ). Areas illuminated by UV light crosslink, while leaving the dark regions un-crosslinked, polymerizing PEGda hydrogel structure. These patterns were irradiated for 10 seconds at a projected UV intensity of ~25 mW cm⁻².

Author contribution

Y.W. synthesized samples, EIS tests, SEM imaging, and analyzed data; P.S. conceived and designed the experiments; Y.X.C. performed DMA tests and cell-culture; S.Y. helped with synthesis and confocal imaging; J.Y. fabricated patterns using stereolithography and imaging with HIROX; P.D. helped with contact angle.

Acknowledgements

We acknowledge Syracuse Biomaterial Institute for providing equipment used for all the experiments in this paper. We thank Dr Jay Henderson's (Professor, Department of Biomedical and Chemical Engineering, Syracuse University) group for their generous donation of 10T1/2 cells, Ciba Specialty Chemicals for donating photoinitiator; the Biology department of Syracuse University for usage of Confocal facility, and Dr Jeremy Gilbert (Professor, Department of Biomedical and Chemical Engineering, Syracuse University) and his PhD students Yangping Liu and Eric Ouellette for training on EIS and SEM respectively.

References

- 1 G. Shi, Z. Zhang and M. Rouabhia, The regulation of cell functions electrically using biodegradable polypyrrole–polylactide conductors, *Biomaterials*, 2008, **29**, 3792–3798.
- 2 A. S. Rowlands and J. J. Cooper-White, Directing phenotype of vascular smooth muscle cells using electrically stimulated conducting polymer, *Biomaterials*, 2008, **29**, 4510–4520.
- 3 S. Sun, I. Titushkin and M. Cho, Regulation of mesenchymal stem cell adhesion and orientation in 3D collagen scaffold by electrical stimulus, *Bioelectrochemistry*, 2006, **69**, 133–141.
- 4 E. Wang, M. Zhao, J. V. Forrester and C. D. McCaig, Bi-directional migration of lens epithelial cells in a physiological electrical field, *Exp. Eye Res.*, 2003, **76**, 29–37.

- 5 S. Sundelacruz, M. Levin and D. L. Kaplan, Membrane potential controls adipogenic and osteogenic differentiation of mesenchymal stem cells, *PLoS One*, 2008, **3**, e3737.
- 6 R. A. Green, N. H. Lovell, G. G. Wallace and L. A. Poole-Warren, Conducting polymers for neural interfaces: challenges in developing an effective long-term implant, *Biomaterials*, 2008, **29**, 3393–3399.
- 7 A. M. Kloxin, M. W. Tibbitt and K. S. Anseth, Synthesis of photodegradable hydrogels as dynamically tunable cell culture platforms, *Nat. Protoc.*, 2010, **5**, 1867–1887.
- 8 K. J. R. Lewis and K. S. Anseth, Hydrogel scaffolds to study cell biology in four dimensions, *MRS Bull.*, 2013, **38**, 260–268.
- 9 M. W. Tibbitt and K. S. Anseth, Hydrogels as extracellular matrix mimics for 3D cell culture, *Biotechnol. Bioeng.*, 2009, **103**, 655–663.
- 10 K. Liu, Y. Li, F. Xu, Y. Zuo, L. Zhang, H. Wang and J. Liao, Graphite/poly(vinyl alcohol) hydrogel composite as porous ringy skirt for artificial cornea, *Materials Science and Engineering: C*, 2009, **29**, 261–266.
- 11 C. J. Ferris, Conducting bio-materials based on gellan gum hydrogels, *Soft Matter*, 2009, **5**, 3430–3437.
- 12 A. K. Gaharwar, N. A. Peppas and A. Khademhosseini, Nanocomposite hydrogels for biomedical applications, *Biotechnol. Bioeng.*, 2014, **111**, 441–453.
- 13 R. A. MacDonald, C. M. Voge, M. Kariolis and J. P. Stegemann, Carbon nanotubes increase the electrical conductivity of fibroblast-seeded collagen hydrogels, *Acta Biomater.*, 2008, **4**, 1583–1592.
- 14 S. Ahadian, J. Ramón-Azcón, M. Estili, X. Liang, S. Ostrovidov, H. Shiku, M. Ramalingam, K. Nakajima, Y. Sakka and H. Bae, Hybrid hydrogels containing vertically aligned carbon nanotubes with anisotropic electrical conductivity for muscle myofiber fabrication, *Sci. Rep.*, 2014, **4**, 4271, DOI: 10.1038/srep04271.
- 15 F. Lamberti, S. Giulitti, M. Giomo and N. Elvassore, Biosensing with electroconductive biomimetic soft materials, *J. Mater. Chem. B*, 2013, **1**, 5083–5091.
- 16 R. Balint, N. J. Cassidy and S. H. Cartmell, Conductive polymers: towards a smart biomaterial for tissue engineering, *Acta Biomater.*, 2014, **10**, 2341–2353.
- 17 S. M. Richardson-Burns, J. L. Hendricks, B. Foster, L. K. Povlich, D.-H. Kim and D. C. Martin, Polymerization of the conducting polymer poly(3,4-ethylenedioxythiophene)(PEDOT) around living neural cells, *Biomaterials*, 2007, **28**, 1539–1552.
- 18 B. D. Malhotra, A. Chaubey and S. Singh, Prospects of conducting polymers in biosensors, *Anal. Chim. Acta*, 2006, **578**, 59–74.
- 19 M. Gizdavic-Nikolaidis, J. Travas-Sejdic, G. A. Bowmaker, R. P. Cooney, C. Thompson and P. A. Kilmartin, The antioxidant activity of conducting polymers in biomedical applications, *Curr. Appl. Phys.*, 2004, **4**, 347–350.
- 20 D. Mawad, E. Stewart, D. L. Officer, T. Romeo, P. Wagner, K. Wagner and G. G. Wallace, A single component conducting polymer hydrogel as a scaffold for tissue engineering, *Adv. Funct. Mater.*, 2012, **22**, 2692–2699.
- 21 T. J. Rivers, T. W. Hudson and C. E. Schmidt, Synthesis of a novel, biodegradable electrically conducting polymer for biomedical applications, *Adv. Funct. Mater.*, 2002, **12**, 33–37.
- 22 E. Kang, K. Neoh and K. Tan, Polyaniline: a polymer with many interesting intrinsic redox states, *Prog. Polym. Sci.*, 1998, **23**, 277–324.
- 23 L. A. Samuelson, A. Anagnostopoulos, K. S. Alva, J. Kumar and S. K. Tripathy, Biologically derived conducting and water soluble polyaniline, *Macromolecules*, 1998, **31**, 4376–4378.
- 24 Y. Cao, P. Smith and A. Heeger, Spectroscopic studies of polyaniline in solution and in spin-cast films, *Synth. Met.*, 1989, **32**, 263–281.
- 25 L. Zhang and M. Wan, Self-Assembly of Polyaniline—From Nanotubes to Hollow Microspheres, *Adv. Funct. Mater.*, 2003, **13**, 815–820.
- 26 M. Li, Y. Guo, Y. Wei, A. G. MacDiarmid and P. I. Lelkes, Electrospinning polyaniline-contained gelatin nanofibers for tissue engineering applications, *Biomaterials*, 2006, **27**, 2705–2715.
- 27 J. Cheung and M. Rubner, Fabrication of electrically conductive Langmuir-Blodgett multilayer films of polyaniline, *Thin Solid Films*, 1994, **244**, 990–994.
- 28 J. Jang, J. Ha and J. Cho, Fabrication of Water-Dispersible Polyaniline-Poly (4-styrenesulfonate) Nanoparticles For Inkjet-Printed Chemical-Sensor Applications, *Adv. Mater.*, 2007, **19**, 1772–1775.
- 29 O. Ngamna, A. Morrin, A. J. Killard, S. E. Moulton, M. R. Smyth and G. G. Wallace, Inkjet printable polyaniline nanoformulations, *Langmuir*, 2007, **23**, 8569–8574.
- 30 T. Dai, X. Qing, J. Wang, C. Shen and Y. Lu, Interfacial polymerization to high-quality polyacrylamide/polyaniline composite hydrogels, *Compos. Sci. Technol.*, 2010, **70**, 498–503.
- 31 M. R. Abidian, D. H. Kim and D. C. Martin, Conducting-Polymer Nanotubes for Controlled Drug Release, *Adv. Mater.*, 2006, **18**, 405–409.
- 32 C. Dispenza, C. L. Presti, C. Belfiore, G. Spadaro and S. Piazza, Electrically conductive hydrogel composites made of polyaniline nanoparticles and poly (N-vinyl-2-pyrrolidone), *Polymer*, 2006, **47**, 961–971.
- 33 J. Huang, X. Hu, L. Lu, Z. Ye, Q. Zhang and Z. Luo, Electrical regulation of Schwann cells using conductive polypyrrole/chitosan polymers, *J. Biomed. Mater. Res., Part A*, 2010, **93**, 164–174.
- 34 V. Guarino, M. A. Alvarez-Perez, A. Borriello, T. Napolitano and L. Ambrosio, Conductive PANi/PEGDA macroporous hydrogels for nerve regeneration, *Adv. Healthcare Mater.*, 2013, **2**, 218–227.
- 35 J. Lin, Q. Tang, J. Wu and Q. Li, A multifunctional hydrogel with high-conductivity, pH-responsive, and release properties from polyacrylate/polypyrrole, *J. Appl. Polym. Sci.*, 2010, **116**, 1376–1383.
- 36 Q. Tang, J. Wu, H. Sun, J. Lin, S. Fan and D. Hu, Polyaniline/polyacrylamide conducting composite hydrogel with a porous structure, *Carbohydr. Polym.*, 2008, **74**, 215–219.
- 37 S. Nemir and J. L. West, Synthetic materials in the study of cell response to substrate rigidity, *Ann. Biomed. Eng.*, 2010, **38**, 2–20.

- 38 L. Ghasemi-Mobarakeh, M. P. Prabhakaran, M. Morshed, M. H. Nasr-Esfahani and S. Ramakrishna, Electrical stimulation of nerve cells using conductive nanofibrous scaffolds for nerve tissue engineering, *Tissue Eng., Part A*, 2009, **15**, 3605–3619.
- 39 P. Humpolicek, V. Kasparkova, P. Saha and J. Stejskal, Biocompatibility of polyaniline, *Synth. Met.*, 2012, **162**, 722–727.
- 40 P. R. Bidez, S. Li, A. G. MacDiarmid, E. C. Venancio, Y. Wei and P. I. Lelkes, Polyaniline, an electroactive polymer, supports adhesion and proliferation of cardiac myoblasts, *J. Biomater. Sci., Polym. Ed.*, 2006, **17**, 199–212.
- 41 P. B. Malafaya and R. L. Reis, Bilayered chitosan-based scaffolds for osteochondral tissue engineering: Influence of hydroxyapatite on *in vitro* cytotoxicity and dynamic bioactivity studies in a specific double-chamber bioreactor, *Acta Biomater.*, 2009, **5**, 644–660.
- 42 G.-I. Im, J.-H. Ahn, S.-Y. Kim, B.-S. Choi and S.-W. Lee, A Hyaluronate-atelocollagen/beta-TCP-hydroxyapatite biphasic scaffold for the repair of osteochondral defects: a porcine study, *Tissue Eng., Part A*, 2009, **16**, 1189–1200.
- 43 S. H. Oh, I. K. Park, J. M. Kim and J. H. Lee, *In vitro* and *in vivo* characteristics of PCL scaffolds with pore size gradient fabricated by a centrifugation method, *Biomaterials*, 2007, **28**, 1664–1671.
- 44 Y. Zhang, J. R. Venugopal, A. El-Turki, S. Ramakrishna, B. Su and C. T. Lim, Electrospun biomimetic nanocomposite nanofibers of hydroxyapatite/chitosan for bone tissue engineering, *Biomaterials*, 2008, **29**, 4314–4322.
- 45 J.-H. Song, H.-E. Kim and H.-W. Kim, Electrospun fibrous web of collagen-apatite precipitated nanocomposite for bone regeneration, *J. Mater. Sci.: Mater. Med.*, 2008, **19**, 2925–2932.
- 46 C. Sun, N. Fang, D. Wu and X. Zhang, Projection micro-stereolithography using digital micro-mirror dynamic mask, *Sens. Actuators, A*, 2005, **121**, 113–120.
- 47 A. Limaye and D. Rosen, Process planning method for mask projection micro-stereolithography, *Rapid Prototyping Journal*, 2007, **13**, 76–84.
- 48 Y. Lu and S. Chen, Direct write of microlens array using digital projection photopolymerization, *Appl. Phys. Lett.*, 2008, **92**, 041109.
- 49 C. Zhou, Y. Chen, Z. Yang and B. Khoshnevis, Digital material fabrication using mask-image-projection-based stereolithography, *Rapid Prototyping Journal*, 2013, **19**, 153–165.
- 50 F. P. W. Melchels, K. Bertoldi, R. Gabbrielli, A. H. Velders, J. Feijen and D. W. Grijpma, Mathematically defined tissue engineering scaffold architectures prepared by stereolithography, *Biomaterials*, 2010, **31**, 6909–6916.
- 51 S. Park, G. Kim, Y. C. Jeon, Y. Koh and W. Kim, 3D polycaprolactone scaffolds with controlled pore structure using a rapid prototyping system, *J. Mater. Sci.: Mater. Med.*, 2009, **20**, 229–234.
- 52 L. Liu, Z. Xiong, Y. Yan, R. Zhang, X. Wang and L. Jin, Multinozzle low-temperature deposition system for construction of gradient tissue engineering scaffolds, *J. Biomed. Mater. Res., Part B*, 2009, **88**, 254–263.
- 53 D. W. Huttmacher, Scaffolds in tissue engineering bone and cartilage, *Biomaterials*, 2000, **21**, 2529–2543.